Ain Shams Engineering Journal (2016) xxx, xxx–xxx

Ain Shams University
Ain Shams Engineering Journal
www.elsevier.com/locate/asej
www.sciencedirect.com

ENGINEERING PHYSICS AND MATHEMATICS

MHD natural convection flow of viscoelastic fluid over an accelerating permeable surface with thermal radiation and heat source or sink: Spectral Homotopy Analysis Approach

A.I. Fagbade *, **B.O. Falodun**, **A.J. Omowaye**

Department of Mathematical Sciences, Federal University of Technology, P.M.B 704, Akure, Ondo State, Nigeria

Received 19 November 2015; revised 4 April 2016; accepted 29 April 2016

KEYWORDS

MHD natural convection;
Thermal radiation;
Viscoelastic fluid;
Heat source;
Spectral Homotopy Analysis Method

Abstract An analysis is presented to study the effects of viscous dissipation and viscoelastic parameter on MHD natural convection flow of viscoelastic fluid over an accelerating permeable surface with thermal radiation and heat source/sink. The governing differential equations that are highly nonlinear are transformed by similarity variables and solved using Spectral Homotopy Analysis Method (SHAM). The effects of various pertinent parameters on the velocity and temperature profiles as well as the skin friction coefficient and the local Nusselt number are presented graphically and in tabular form. The SHAM results are compared favorably with already established results in literatures. It is found that the magnetic field acts as a retarding force on the velocity profile of the flow but has a propelling effect on the thermal condition of the flow. It was revealed that an increase in thermal radiation parameter of the flow produces significant increase in the thermal condition of the fluid temperature.

1. Introduction

Natural convection flow under the influence of gravitational force has been investigated most extensively because they occur frequently in nature as well as in science and engineering applications. When a heated surface is in contact with a fluid, the result of temperature difference causes buoyancy force, which induces the natural convection. Recently heat flux applications are widely used in industries, engineering and science fields. Heat flux sensors can be used in industrial measurement and control systems. Examples of few applications are detection fouling (Boiler Fouling Sensor), monitoring of furnaces

* Corresponding author.
E-mail addresses: aifagbade@futa.edu.ng (A.I. Fagbade), falodunbidemi2014@gmail.com (B.O. Falodun), ajomowaye@futa.edu.ng (A.J. Omowaye).

Peer review under responsibility of Ain Shams University.

Production and hosting by Elsevier

http://dx.doi.org/10.1016/j.asej.2016.04.021
2090-4479 © 2016 Faculty of Engineering, Ain Shams University. Production and hosting by Elsevier B.V.

Please cite this article in press as: Fagbade AI et al., MHD natural convection flow of viscoelastic fluid over an accelerating permeable surface with thermal radiation and heat source or sink: Spectral Homotopy Analysis Approach, Ain Shams Eng J (2016), http://dx.doi.org/10.1016/j.asej.2016.04.021

(Blast Furnace Monitoring/General Furnace Monitoring) and flare monitoring. Use of heat flux sensors can lead to improvements in efficiency, system safety and modeling. Chen [1] performed an analysis to study the natural convection flow over a permeable inclined surface with variable wall temperature and concentration. The results show that the flow velocity reduces in the presence of a magnetic field and establishes that an increase in the angle of inclination between the flow and the surface lowers the effect of buoyancy force but boosts the heat transfer rate at a significant value of Prandtl number. Ezzat et al. [2] studied combined heat and mass transfer for unsteady MHD flow of perfect conducting micropolar fluid with thermal relaxation. In their analysis, Laplace transform techniques were applied to a thermal–chemical reactive shock problem in a half space. They presented numerical results for the temperature, velocity, concentration, microrotation and induced magnetic field distributions. Kalpadides and Balassas [3] studied free convective boundary layer problem of an electrically conducting fluid over an elastic surface using group theoretic method. They obtained a standard result which agreed with the existing results in the literature for the group of scaling symmetry. Ibrahim et al. [4] investigated the similarity reductions for problem of radiative and magnetic field effects on free convection and mass-transfer flow past a semi-infinite flat plate. They obtained new similarity reductions and found an analytical solution for the uniform magnetic field by using Lie group method and presented the numerical analysis on the influence of non-uniform magnetic field.

The role of thermal radiation on the flow and heat transfer process is of major importance in the design of many advanced energy conversion systems operating at higher temperature e.g. Nuclear power plants, gas turbines and various propulsion devices for aircraft, missiles, satellites and space vehicles. Thermal radiation within this system is usually as a result of emission by hot walls and the working fluid Seigel and Howell [5]. In the similar input, Effect of thermal radiation and soret in the presence of heat source/sink on unsteady MHD flow past a semi-infinite vertical plate was studied by Srihari and Srinivas [6]. Non-aligned MHD stagnation point flow of variable viscosity nanofluids past a stretching sheet with radiative heat was investigated by Waqar et al. [7]. They transformed the governing nonlinear partial differential equations into a set of nonlinear ordinary differential equations using similarity transformation and solved by fourth–fifth order Runge–Kutta–Tehlberg method. It was found that non-alignment of the re-attachment point on the sheet surface decreases with increase in magnetic field intensity. Makinde et al. [8] discussed the MHD variable viscosity reacting flow over a convectively heated plate in a porous medium with thermophoresis and radiative heat transfer. The system of nonlinear ordinary differential equations governing the flow is solved numerically using the Nachtsheim and Swigert shooting iteration technique together with a sixth-order Runge–Kutta iteration algorithm. Free convection effects on perfectly conducting fluid were studied by Magdy [9]. It was noticed that in both cooling and heating of the surface as Alfven velocity increases, the velocity of the flow reduces significantly. They explained that this may be due to the fact that the effect of the magnetic field corresponds to a term signifying a positive force that tends to decelerate the fluid particles.

Recently, many researchers have looked into the qualitative influence of variable heat source, mass transfer coefficient, thermal radiation and heat source or sink in various physical geometry of the flow. Important in this regard is the research work of Chamkha and Ahmed [10], Seth et al. [11], Das et al. [12] and Raju et al. [13]. For instance, Sharma and Singh [14] examined the effects of variable thermal conductivity and heat source/sink on MHD flow near a stagnation point on a linearly stretching sheet. Fagbade et al. [15] delved into the influence of magnetic field, viscous dissipation and thermophoresis on Darcy–Forcheimer mixed convection flow in fluid saturated porous media. In the study, the similarity variable is used to transform the governing equations into a boundary valued problem of coupled ordinary differential equations and solved by Spectral Homotopy Analysis Method (SHAM). Waqar et al. [16] discussed the combined heat and mass transfer of third-grade nanofluids over a convectively-heated stretching permeable surface. They converted the partial differential equation of the model into ordinary differential equation using the similarity variables and observed that viscoelastic parameter has a tendency to lower the flow velocity and temperature but increases the dimensionless concentration at the surface.

Viscoelastic flows and transport phenomena arise in numerous areas of chemical, industrial process, biosystems, food processing and biomedical engineering. These include the rheology of liquid crystal precursors employed in the manufacture of carbon super fibers, crude oil emulsion processing, paper coating rheological processing, propulsive ciliary transport of respiratory airway mucus, thermo-capillary bubble dynamics in weakly elastic fluids, rhe-reactor phosphatation flows, flour rheology, mayonnaise elastic–viscous flows, xanthan gum hydrogel flows, and polygalacturonase-based food stuff. Ezzat and Abd-Elaal [17] studied the state space approach to viscoelastic fluid flow of hydromagnetic fluctuating boundary-layer through a porous medium. They obtained the solution to a problem of an electrically conducting viscoelastic fluid in the presence of a transverse magnetic field between two parallel fixed plates. Makanda et al. [18] studied the natural convection of viscoelastic fluid from a cone embedded in a porous medium with viscous dissipation using successive linearization method (SLM).

Magdy and Abd-Elaal [19] discussed free convection effects on a viscoelastic boundary layer flow with one relaxation time through a porous medium. The discussion of the effects of cooling and heating on a viscoelastic conducting fluid was given. They found out that for large values of the permeability of the porous medium, the velocity inside the boundary layer increases to a value greater than the free stream velocity and then levels off gradually to reach the value of the free stream outside the boundary layer. Prasad et al. [20] discussed the characteristics of heat transfer and momentum in an incompressible electrically conducting non-Newtonian boundary layer flow of a viscoelastic fluid over a stretching sheet. They assumed that the fluid viscosity and thermal conductivity vary as an inverse and linear thermal conductivity respectively. It was also found that there was a significant decrease in wall temperature profile and skin friction of the sheet by increasing magnetic field parameter.

The objective of the present paper was to investigate MHD natural convective flow of non-Newtonian fluid characterized by Walter's B liquid with heat transfer in the presence of thermal radiation and heat source/sink over an accelerating permeable surface with a view to understudy the influence of viscoelastic effects and viscous dissipation on the flow.

Please cite this article in press as: Fagbade AI et al., MHD natural convection flow of viscoelastic fluid over an accelerating permeable surface with thermal radiation and heat source or sink: Spectral Homotopy Analysis Approach, Ain Shams Eng J (2016), http://dx.doi.org/10.1016/j.asej.2016.04.021

2. Mathematical formulation

Consider a steady, laminar and two dimensional flow of an incompressible Walters liquid B fluid over an accelerating permeable surface coinciding with a plane $y = 0$ and the flow being confined to $y > 0$. The flow is generated due to the stretching of the surface, caused by the simultaneous application of a magnetic field of uniform strength B_0 executed in the direction of y-axis. The magnetic reynolds number is assumed to be small and that the induced magnetic field is neglected. The surface is assumed to be permeable so as to allow possible wall fluid suction or injection with significant consideration for thermal radiation and buoyancy effects. We take y-axis along the surface, x-axis being normal to it and u and v are the fluid tangential velocity and normal velocity, respectively as shown in Fig. 1. The model of Walters B fluid is chosen for our study as it involves only one non-Newtonian parameter. The Cauchy stress tensor S in such a fluid is related to the motion in the following manner, Mehmood [21]:

$$S = -PI + \tau, \tag{1}$$

$$\tau = 2\eta_0 e - 2k_0 \frac{\delta e}{\delta t}, \tag{2}$$

where P is the fluid pressure, I is the identity tensor and the rate of strain tensor e is defined by:

$$2e = \nabla(\underline{v}) + \nabla(\underline{v})^T. \tag{3}$$

where v is the velocity vector, ∇ is the gradient operator and $\frac{\delta}{\delta t}$ denotes the convected differentiation of a tensor quantity in relation to the material in motion. The convected differentiation of the rate of strain tensor is given by:

$$\frac{\delta e}{\delta t} = \frac{\partial e}{\partial t} + \underline{v} \cdot \nabla(e) - e \cdot \nabla(\underline{v}) - (\nabla(\underline{v}))^T \cdot e \tag{4}$$

The limiting viscosity η_0 at small rate of shear and the short memory coefficient k_0 for the Walter's B fluid are defined by:

$$\eta_0 = \int_0^\infty \lambda(\varsigma) d\varsigma, \tag{5}$$

$$k_0 = \int_0^\infty \tau\lambda(\varsigma) d\varsigma. \tag{6}$$

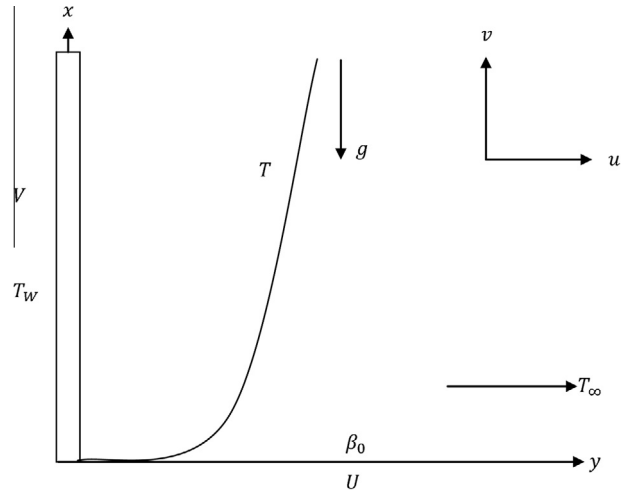

Figure 1 Flow configuration and coordinate system.

where $\lambda(\varsigma)$ being the relaxation spectrum as introduced by Walters [22]. This idealized model is a valid approximation of Walters B fluid taking very short memory into account so that terms involving

$$\int_0^\infty \tau^n \lambda(\tau) d\tau \quad n \geqslant 2. \tag{7}$$

have been neglected.

As a result of the above simplifications, assumptions and Boussineq's approximation, the governing equations, modeling the flow of Walter's B fluid through a permeable surface following Chamkha [23] can be written as:

$$\frac{\partial u}{\partial x} + \frac{\partial v}{\partial y} = 0, \tag{8}$$

$$u\frac{\partial u}{\partial x} + v\frac{\partial u}{\partial y} = \frac{\partial \tau_{xx}}{\partial x} + \frac{\partial \tau_{xy}}{\partial y} + g\beta(T - T_\infty) - \frac{\sigma B_0^2 u}{\rho}, \tag{9}$$

$$u\frac{\partial T}{\partial x} + v\frac{\partial T}{\partial y} = K\frac{\partial^2 T}{\partial y^2} + \frac{1}{\rho c_p} tr(\tau.L) + \frac{\beta^* u}{\rho c_p}(T_\infty - T) + \frac{Q_0}{\rho c_p}(T - T_\infty) + \frac{\sigma B_0^2}{\rho c_p} u^2 - \frac{1}{\rho c_p}\frac{\partial q_r}{\partial y}. \tag{10}$$

With

$$L = \nabla(\underline{v}), \tag{11}$$

$$\tau = \begin{pmatrix} \tau_{xx} & \tau_{xy} \\ \tau_{yx} & \tau_{yy} \end{pmatrix}, \tag{12}$$

$$\tau_{xx} = 2\eta_0 u_x - 2k_0\left[uu_{xx} + vu_{xy} - 2u_x^2 - u_y v_x - v_x^2\right], \tag{13}$$

$$\tau_{xy} = \tau_{yx} = \eta_0(u_y + v_x) - 2k_0\left[\frac{1}{2}uu_{xy} + \frac{1}{2}uv_{xx} + \frac{1}{2}vu_{yy} + \frac{1}{2}vv_{xy} - \frac{3}{2}u_x u_y - \frac{1}{2}u_y v_y - \frac{1}{2}u_x v_x - v_x v_y\right], \tag{14}$$

$$\tau_{yy} = 2\eta_0 v_y - 2k_0\left[uv_{xy} + vv_{yy} - u_y v_x - u_y^2 - v_y^2\right], \tag{15}$$

$$tr(\tau \cdot L) = \left(u_x\tau_{xx} + v_x\tau_{xy} + u_y\tau_{yx} + v_y\tau_{yy}\right). \tag{16}$$

where x and y are the vertical and horizontal directions respectively. u and v are the fluid velocity components in the x and y directions. ρ is the fluid density, v is the kinematic viscosity, c_p is the specific heat at constant pressure, K is the thermal diffusivity, k is the fluid thermal conductivity, β is the volumetric expansion coefficient, σ is the electric conductivity, B_0 is the applied magnetic induction, q_r is the radiative heat flux, k_0 is the fluid visco-elasticity, T_∞ is the free stream temperature. The terms $\beta^*(T_\infty - T)$ and $Q_0(T - T_\infty)$ represent the heat generation or absorption per unit volume respectively. Similarly, the contribution of thermal radiative heat flux q_r, is based on Rosseland approximation. Rosseland approximation requires that the medium is optically dense and radiation travels only a short distance before being scattered or absorbed. Therefore, a simplified model for Radiative Transfer Equation (RTE) based on Rosseland approximation as noted by Md Miraj et. al. [24] is given as:

$$q_r = -\frac{4\sigma_s}{3k_e}\frac{\partial T^4}{\partial y}, \tag{17}$$

where σ_s is the Stefan–Boltzmann constant and k_e is known as absorption coefficient. We assumed that the temperature difference within the flow regime is sufficiently small such that T^4 can be expressed as a linear function of the free stream temperature T_∞. This is simplified by expanding T^4 in Taylor series about T_∞ and forgone the higher order terms. Considering the Taylor's series expansion of a function $g(x)$ about x_0

$$g(x) = g(x_0) + (x - x_0)g'(x_0) + \frac{(x - x_0)^2}{2!}g''(x_0) + \cdots + \frac{(x - x_0)^n}{n!}g^n(x_0), \tag{18}$$

Likewise, expansion of T^4 about T_∞. Setting $g(x) = T^4$ and $g(x_0) = g(T_\infty) = T_\infty^4$ in above equation. Neglecting higher order, we obtain $T^4 = 4T_\infty^3 T - 3T_\infty^4$. Thus

$$\frac{1}{\rho c_p}\frac{\partial q_r}{\partial y} = -\frac{16\sigma_s T_\infty^3}{3\rho c_p k_e}\frac{\partial^2 T}{\partial y^2}. \tag{19}$$

Using the above simplifications in Eqs. (9) and (10), we have:

$$u\frac{\partial u}{\partial x} + v\frac{\partial u}{\partial y} = v\frac{\partial^2 u}{\partial y^2} - k_0\left[v\frac{\partial^3 u}{\partial y^3} + u\frac{\partial^3 u}{\partial y^2 \partial x} - 2\frac{\partial u}{\partial y}\frac{\partial^2 u}{\partial x \partial y} - 3\frac{\partial u}{\partial x}\frac{\partial^2 u}{\partial y^2}\right] + g\beta(T - T_\infty) - \frac{\sigma B_0^2}{\rho}u, \tag{20}$$

$$u\frac{\partial T}{\partial x} + v\frac{\partial T}{\partial y} = K\frac{\partial^2 T}{\partial y^2} + \frac{16\sigma_s}{3\rho c_p k_e}T_\infty^3\frac{\partial^2 T}{\partial y^2} + \frac{Q_0}{\rho c_p}(T - T_\infty) + \frac{\beta^*}{\rho c_p}(T_\infty - T)u + \frac{1}{\rho c_p}\left[2\eta_0\left(\frac{\partial u}{\partial y}\right)^2 - k_0\left(u\frac{\partial u}{\partial y}\frac{\partial^2 u}{\partial x \partial y} + v\frac{\partial u}{\partial y}\frac{\partial^2 u}{\partial y^2} - 3\frac{\partial u}{\partial x}\left(\frac{\partial u}{\partial y}\right)^2 - 3\frac{\partial v}{\partial y}\left(\frac{\partial u}{\partial y}\right)^2\right)\right] + \frac{\sigma B_0^2}{\rho c_p}u^2. \tag{21}$$

subject to the following boundary conditions:

$$u(x,0) = ax, \quad v(x,0) = v_w, \quad T(x,0) = T_w(x) = T_\infty + A_0 x, \quad u(x,\infty) = 0, \quad T(x,\infty) = T_\infty. \tag{22}$$

where a is the stretching rate (a constant), v_w is the wall suction velocity when $(v_w > 0)$ or injection when $(v_w < 0)$, and $T_w(x)$ is the wall temperature.

It is worth noting that the physical quantities of engineering interest in this problem are skin-friction coefficient C_f and local Nusselt number Nu defined respectively as:

$$C_f = \frac{\tau_w}{\eta_0\left(\sqrt{\frac{a}{v}}\right)ax}. \tag{23}$$

$$Nu = \frac{vq_w}{Ka(T_w - T_\infty)}. \tag{24}$$

With respect to the Walter's B memory fluid and radiative transfer equation (RTE) based on Rosseland approximation, the corresponding wall shear stress (τ_w) and the rate of heat transfer q_w are derived as:

$$\tau_w = \tau_{xy} = \eta_0\frac{\partial u}{\partial y} - k_0\left[u\frac{\partial^2 u}{\partial y \partial x} - 3\frac{\partial u}{\partial x}\frac{\partial u}{\partial y}\right]_{y=0}, \tag{25}$$

$$q_w = -K\left(\frac{\partial T}{\partial y}\right)_{y=0} - \frac{4\sigma_s}{3k_e}\left(\frac{\partial T^4}{\partial y}\right)_{y=0}. \tag{26}$$

Using the following similarity transformation:

$$\psi = (va)^{\frac{1}{2}}xf(\eta), \quad \eta = \left(\frac{a}{v}\right)^{\frac{1}{2}}y, \quad u = \frac{\partial \psi}{\partial y}, \quad v = -\frac{\partial \psi}{\partial y}. \quad T = T_\infty + (T_w - T_\infty)\theta(\eta). \tag{27}$$

where $\psi(x,y)$ is the stream function introduced to ensure that continuity equation is satisfied. Hence, the transformed governing equation is obtained as

$$f''' + ff'' + \alpha(ff^{iv} + f'f''' + 2f''^2 - f'f'') - Mf' - f'^2 + Gr\theta = 0, \tag{28}$$

$$\left(\frac{1+R}{Pr}\right)\theta'' + f\theta' - f'\theta(1 + d_y) + \Delta\theta + EcMf'^2 + 2Ecf''^2 + Ec\alpha\left[ff''f''' - f'f''^2\right] = 0. \tag{29}$$

Subject to the following boundary conditions:

$$f'(0) = 1, \quad f(0) = -\beta_0, \quad \theta(0) = 1, \tag{30}$$

$$f'(\infty) = 0, \quad \theta(\infty) = 0. \tag{31}$$

Note: $\beta_0 = \frac{v_w}{(av)^{\frac{1}{2}}}$ is the wall mass transfer coefficient such that $\beta_0 > 0$ denotes wall suction and $\beta_0 < 0$ corresponds to wall blowing conditions. Where

$$Ec = \frac{(ax)^2}{c_p(T_w - T_\infty)}, \quad M = \frac{\sigma B_0^2}{a\rho}, \quad Gr = \frac{g\beta\theta(T_w - T_\infty)}{a^2 x}, \quad \alpha = \frac{k_0 a}{v}, \quad \beta_0 = \frac{v_w}{(av)^{\frac{1}{2}}}, \quad \Delta = \frac{Q_0}{\rho c_p a}, \quad Pr = \frac{v}{\alpha}, \quad R = \frac{16\sigma_s T_\infty^3}{3k_e K}, \quad d_y = \frac{\beta^* x}{\rho c_p}.$$

are the Eckert number, Hartmann number, Thermal Grashof number, The viscoelastic parameter or Weissenberg number, the wall mass transfer coefficient, heat source/sink parameter, Prandtl number, thermal radiation parameter and internal heat generation/absorption coefficient parameter respectively. Similarly, by using the similarity variable introduced earlier on the above physical quantities of engineering application, we obtain:

$$C_f = f''(0) + 2\alpha f'(0)f''(0), \tag{32}$$

$$Nu = -\theta'(0)(1 + R). \tag{33}$$

It is seen that C_f and Nu are directly proportional to the wall velocity and temperature gradients, respectively.

3. Spectral Homotopy Analysis Method

The use of the Chebyshev spectral collocation method is now becoming the preferred tool for solving ordinary and partial differential equations because of their elegance and high accuracy in resolving problems with smooth functions. In applying the Spectral-Homotopy Analysis Method, it is convenient to first transform the domain of the problem from $[0, \infty]$ to $[-1, 1]$ and make the governing boundary conditions homogeneous by using the transformations.

Please cite this article in press as: Fagbade AI et al., MHD natural convection flow of viscoelastic fluid over an accelerating permeable surface with thermal radiation and heat source or sink: Spectral Homotopy Analysis Approach, Ain Shams Eng J (2016), http://dx.doi.org/10.1016/j.asej.2016.04.021

Table 1 Comparison of wall temperature gradient $(-\theta' f(0))$ with results reported by Chamkha [10] and Acharya et al. [25] when $Pr = 0.71$, $\alpha = Gr = R = M = \Delta = 0$.

	$\beta_0 = 0.45$ $d_y = 0.5$	$\beta_0 = 0.45$ $d_y = 1.0$	$\beta_0 = 0$ $d_y = 0.5$	$\beta_0 = 0$ $d_y = 1.0$	$\beta_0 = -1.5$ $d_y = 0.5$	$\beta_0 = -1.5$ $d_y = 1.0$
Present work	0.82148	0.96253	0.94987	1.07797	1.57179	1.66954
Chamkha [10]	0.82397	0.96191	0.94769	1.07996	1.57077	1.66184
Acharya et al. [25]	0.82250	0.96180	0.94620	1.07890	1.56960	1.66030

Table 2 Computed values of skin friction coefficient C_f and local Nusselt number at different values of viscoelastic parameter α and Magnetic parameter M when $Pr = 0.71$, $Gr = 0.5$, $Ec = 0.01$, $\Delta = 0$.

α	M	$\beta_0 = -0.5,\ R = 0$		$\beta_0 = 0,\ R = 0$		$\beta_0 = 0.5,\ R = 0$		$\beta_0 = -0.5,\ R = 0.5$		$\beta_0 = 0,\ R = 0.5$	
		C_f	Nu	C_f	Nu	C_f	$Nu(0)$	C_f	Nu	C_f	Nu
0	0	1.02012	1.12032	0.61343	0.96393	0.11318	0.85134	0.91361	1.29474	0.45788	1.15242
	0.5	1.59439	1.03511	1.22837	0.87029	0.76919	0.74029	1.51806	1.18593	1.12882	1.01474
	1.0	2.08219	0.97811	1.74978	0.80524	1.33754	0.65143	2.02395	1.11387	1.67946	0.92332
0.01	0	1.02979	1.12070	0.56275	0.96834	0.01305	0.85796	0.91276	1.29609	0.39329	1.15842
	0.5	1.71062	1.02916	1.27428	0.86899	0.75397	0.74238	1.62715	1.17996	1.16601	1.01388
	1.0	2.29355	0.96779	1.88167	0.79981	1.39951	0.64977	2.23022	1.10285	1.80546	0.91748

$$\xi = \frac{2\eta}{L} - 1, \quad \xi\epsilon[-1, 1] \tag{34}$$

$$f(\eta) = f(\xi) + f_0(\eta), \quad \theta(\eta) = \theta(\xi) + \theta_0(\eta). \tag{35}$$

$$f_0(\eta) = 1 + \beta_0 - e^{-\eta}, \quad f_0'(\eta) = e^{-\eta}, \quad \theta_0(\eta) = e^{-\eta} \tag{36}$$

Substituting Eq. (35) above into the transformed governing Eqs. (28), (29) and boundary condition (30), (31) gives:

$$\begin{aligned} &f'''(\xi) + \alpha a_1 f(\xi) + \alpha a_2 f^{iv}(\xi) + 2\alpha a_5 f'(\xi) - Mf'(\xi) + 2\alpha a_4 f''' \\ &\quad + a_3 f + a_2 f''(\xi) - 2a_4 f'(\xi) + Gr\theta(\xi) + \alpha f(\xi) f'''(\xi) \\ &\quad + 2\alpha f'(\xi) f'''(\xi) - f'^2(\xi) + f(\xi) f''(\xi) + 2\alpha f''(\xi)^2 \\ &\quad + 4\alpha a_3 f''(\xi) = H_1(\eta), \end{aligned} \tag{37}$$

$$\begin{aligned} &\frac{1}{Pr}(1+R)\theta''(\xi) + b_1 f(\xi) + b_2\theta'(\xi) - b_3 f'(\xi) - b_4\theta(\xi) \\ &- d_y b_3 f'(\xi) - d_y b_4\theta(\xi) + \Delta\theta(\xi) + f(\xi)\theta'(\xi) - f'(\xi)\theta(\xi) \\ &- d_y f'(\xi)\theta(\xi) + 2EcMa_4 f'(\xi) + EcMf'^2(\xi) + 2Ecf''^2(\xi) \\ &- Ec\alpha f'(\xi) f''^2(\xi) - 2Eca_3\alpha f'(\xi) f''(\xi) - Ec\alpha a_3^2 f'(\xi) \\ &- Ec\alpha a_4 f''^2(\xi) - 2Ec\alpha a_4 a_3 f''(\xi) + Ec\alpha f(\xi) f''(\xi) f'''(\xi) \\ &+ Ec\alpha a_5 f(\xi) f''(\xi) + Ec\alpha a_4 f(\xi) f'''(\xi) + Ec\alpha a_4 a_5 f(\xi) \\ &+ Ec\alpha a_2 f''(\xi) f'''(\xi) + Ec\alpha a_2 a_5 f''(\xi) + Ec\alpha a_2 a_4 f'''(\xi) = H_2(\eta). \end{aligned} \tag{38}$$

Subject to:

$$f(-1) = f'(-1) = f'(1) = 0, \quad \theta(-1) = \theta(1) = 0. \tag{39}$$

where the prime denotes differentiation with respect to ξ and has set

$$\begin{aligned} &a_1 = f_0'''(\eta), \quad a_2 = f_0(\eta), \quad a_3 = f_0''(\eta), \quad a_4 = f_0'(\eta) \\ &b_1 = \theta_0'(\eta), \quad b_2 = f_0(\eta), \quad b_3 = \theta_0(\eta), \quad b_4 = f_0'(\eta). \end{aligned} \tag{40}$$

And

$$\begin{aligned} H_1(\eta) = &-f_0'''(\eta) - f_0(\eta) f_0''(\eta) + f_0'^2(\eta) + Mf_0'(\eta) - 2\alpha f_0'(\eta) f_0'''(\eta) \\ &- Gr\theta_0(\eta) - \alpha f_0(\eta) f_0^{iv}(\eta) - 2\alpha f_0''(\eta), \end{aligned} \tag{41}$$

$$\begin{aligned} H_2(\eta) = &-\frac{1}{Pr}(1+R)\theta_0''(\eta) - \theta_0'(\eta) f_0(\eta) - f_0'(\eta)\theta_0(\eta) \\ &+ d_y f_0'(\eta)\theta_0(\eta) - \Delta\theta_0(\eta) - EcMf_0'^2(\eta) - 2Ecf_0''^2(\eta) \\ &+ Ec\alpha f_0'(\eta) f_0''^2(\eta) - Ec\alpha f_0(\eta) f_0'(\eta) f_0'''(\eta). \end{aligned} \tag{42}$$

The non-homogeneous linear part of the governing Eqs. (37) and (38) is given by

$$\begin{aligned} &f_l''' + \alpha a_1 f_l + \alpha a_2 f_l^{iv} + 2\alpha a_5 f_l' - Mf_l' + 2\alpha a_4 f_l''' + a_3 f_l + a_2 f_l'' \\ &\quad - 2a_4 f_l' + Gr\theta_l + 4\alpha a_3 f_l'' = H_1(\eta), \end{aligned} \tag{43}$$

$$\begin{aligned} &\frac{1}{Pr}(1+R)\theta_l'' + b_1 f_l + b_2\theta_l' - b_3 f_l' - b_4\theta_l - d_y b_3 f_l' - d_y b_4\theta_l + \Delta\theta_l \\ &\quad + 2EcMa_4 f_l' + 4Eca_3 f_l'' - 2Ec\alpha a_3^2 f_l' - 2Ec\alpha a_3 a_4 f_l'' + Ec\alpha a_5 a_4 f_l \\ &\quad + Ec\alpha a_2 a_5 f_l'' + Ec\alpha a_2 a_4 f_l''' = H_2(\eta). \end{aligned} \tag{44}$$

Subject to:

$$f_l'(-1) = f_l'(1) = 0, \quad \theta_l(-1) = \theta_l(1) = 0, \quad f_l(-1) = f_l(1) = 0. \tag{45}$$

The Chebyshev pseudospectral method is used to solve (43) and (44) and the unknown functions $f_l(\xi)$ and $\theta_l(\xi)$ are approximated as a truncated series of Chebyshev polynomials of the form

$$f_l(\xi) \approx f_l^N = \sum_{k=0}^{N} f_k^N T_{11k}(\xi_J) \quad J = 0, 1, 2, \ldots, N \tag{46}$$

$$\theta_l(\xi) \approx \theta_l^N = \sum_{k=0}^{N} \theta_k^N T_{21k}(\xi_J) \quad J = 0, 1, 2, \ldots, N \tag{47}$$

where T_{1k} and T_{2k} are the kth Chebyshev polynomials with coefficients f_k, θ_k respectively and $\xi_0, \xi_1, \xi_2, \ldots, \xi_N$ are Gauss–Lobatto collocation point defined by

$$\xi_J = \cos\left(\frac{\pi J}{N}\right) \quad J = 0, 1, 2, \ldots, N, \tag{48}$$

Table 3 Computed values of skin friction coefficient C_f and local Nusselt number at different values of viscous dissipation term Ec and thermal Grashof number Gr when $Pr = 0.71$, $R = 0.5$, $M = 0.5$, $\beta_0 = 0.45$, $\alpha = 0.01$, $\delta_y = 0.5$.

Ec	Gr	$\Delta = -1$		$\Delta = 0$	
		C_f	Nu	C_f	Nu
0.01	0	1.38256	1.37992	1.38256	0.85704
	0.5	1.01082	1.41622	0.81963	0.97228
	2.0	0.00416	1.50892	0.40836	1.16864
0.1	0	1.38256	1.34002	1.38256	0.81588
	0.5	1.00491	1.36533	0.78928	0.89384
	2.0	0.07102	1.43484	0.63153	1.05327

where N is the number of collocation points. The derivatives of the function $f_l(\xi)$, $\theta_l(\xi)$ at the collocation points are presented as;

$$\frac{d^r f_l}{d\xi^r} = \sum_{k=0}^{N} D_{kJ}^r f_l(\xi_J), \quad \frac{d^r \theta_l}{d\xi^r} = \sum_{k=0}^{N} D_{kJ}^r \theta_l(\xi_J), \tag{49}$$

where r is the order of differentiation and $\mathbf{D} = \frac{2}{L}D$ and D is the Chebyshev spectral differentiation matrix. Substituting Eqs. (46)–(49) into Eqs. (43) and (44), we obtain

$$\mathbf{AF_L} = \mathbf{G} \tag{50}$$

Subject to

$$f_l(\xi_N) = -\beta_0, \quad \sum_{k=0}^{N} D_{Nk} f_k(\xi_k) = 1, \quad \sum_{k=0}^{N} D_{0k} f_k(\xi_k) = 0,$$
$$\theta_l(\xi_N) = 1, \quad \theta_l(\xi_0) = 0. \tag{51}$$

where

$$\mathbf{A} = \begin{pmatrix} A_{11} & A_{12} \\ A_{21} & A_{22} \end{pmatrix}, \tag{52}$$

$$A_{11} = D^3 + \alpha a_1 I + a_2 D^2 - 2a_4 D - MD + 2\alpha a_4 D^3 + 2\alpha a_5 D + \alpha a_2 D^4 + 4\alpha_3 D^2 \tag{53}$$

$$A_{12} = GrI, \quad A_{22} = \frac{1}{Pr}(1+R)D^2 + D + b_2 D - b_4 D - d_y b_4 I + \Delta I,$$
$$A_{21} = b_1 - b_3 D - d_y b_3 D + 2EcMa_4 D + 4Eca_3 D^2 - Ec\alpha a_3^2 D - 2Ec\alpha a_3 a_4 D^2 + 2Ec\alpha a_4 a_5 D + Ec\alpha a_2 a_5 D^2 + 2Ec\alpha a_2 a_4 D^3$$
$$F_l = [f_l(\xi_0), \ldots, f_l(\xi_N), \theta_l(\xi_0), \ldots, \theta_l(\xi_N)]$$
$$G = [H_l(\eta_0), \ldots, H_l(\eta_N), H_2(\eta_0), \ldots, H_2(\eta_N)]$$
$$a_i = diag([a_i(\eta_0), \ldots, a_i(\eta_{N-1}), a_i(\eta_{N-1}, a_i(\eta_N])$$
$$b_i = diag([b_i(\eta_0), \ldots, b_i(\eta_{N-1}), b_i(\eta_{N-1}, b_i(\eta_N])\ i = 1,2,3$$

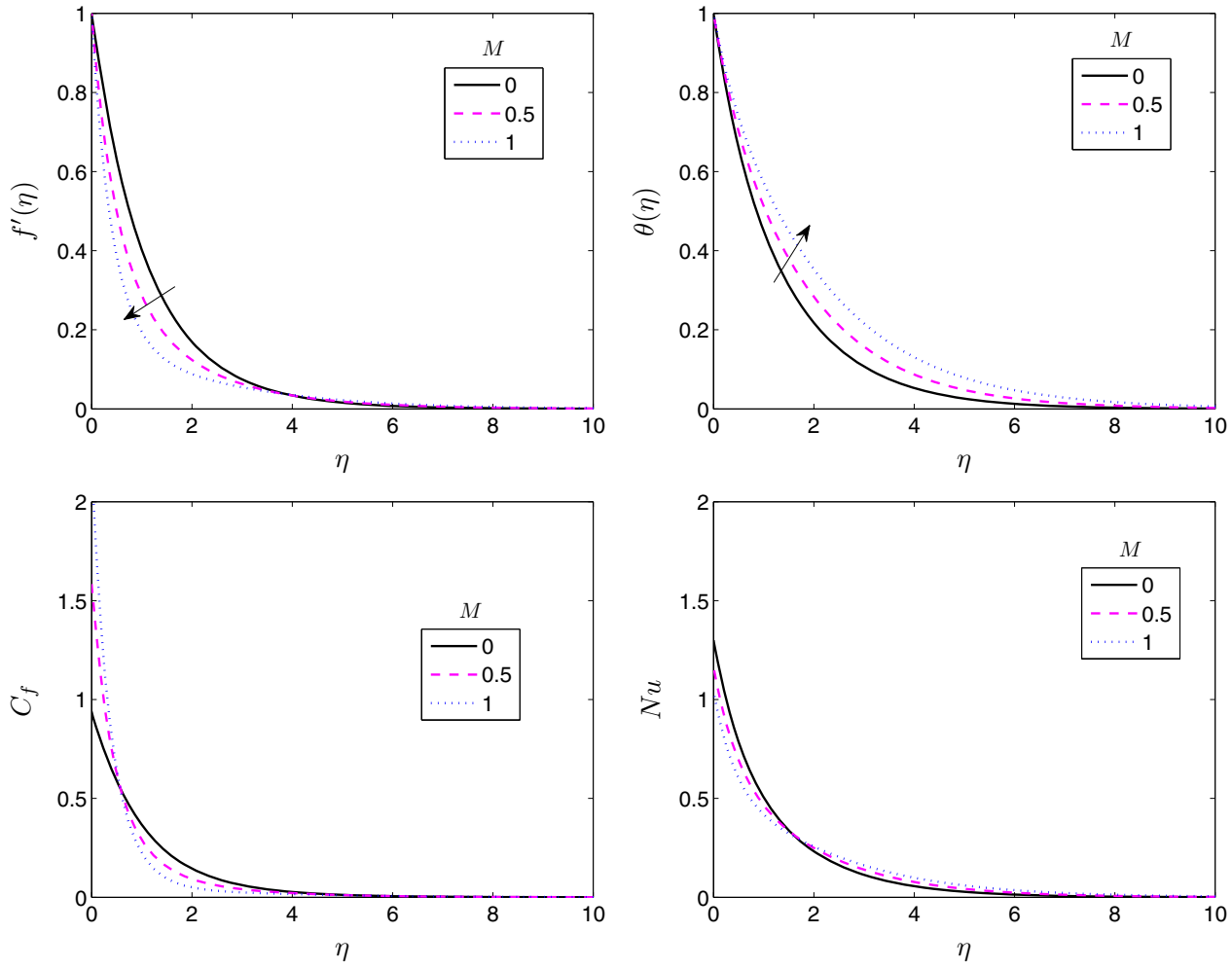

Figure 2 Effect of Hartmann parameter (M) on velocity, temperature, skin friction coefficient and local Nusselt number profiles.

The first and the last rows and columns of A are deleted so as to implement the boundary conditions (51). These boundary conditions are then imposed on the first and last rows of the modified matrix A. Setting the modified matrix G to zero, the values of $f_l(\xi_0),\ldots,f_l(\xi_N)$, $\theta_l(\xi_0),\ldots,\theta_l(\xi_N)$ are then determined from;

$$\mathbf{F_l} = \mathbf{A^{-1}}.\mathbf{G} \tag{54}$$

The above equation provides us with the initial approximation to obtain SHAM solution for the governing equations. We now define the following linear operators to seek for the convergent series of SHAM approximation solutions of (37) and (38) by first defining the following linear operators:

$$\begin{aligned} L_f[\bar{f}(\eta,q),\bar{\theta}(\eta,q)] = {} & f_l''' + \alpha a_1 f_l + \alpha a_2 f_l'''' + 2\alpha a_5 f_l' - M f_l' + 2\alpha a_4 f_l''' \\ & + a_3 f_l + a_2 f_l'' - 2a_4 f_l' + Gr\theta_l + 4\alpha a_3 f_l'', \end{aligned} \tag{55}$$

$$\begin{aligned} L_\theta[\bar{f}(\eta,q),\bar{\theta}(\eta,q)] = {} & \frac{1}{Pr}(1+R)\theta_l'' + b_1 f_l + b_2\theta_l' - b_3 f_l' \\ & - b_4\theta_l - d_y b_3 f_l' - d_y b_4\theta_l + \Delta\theta_l \\ & - 2Ec\alpha a_3^2 f_l' - 2Ec\alpha a_3 a_4 f_l'' \\ & + Ec\alpha a_5 a_4 f_l + Ec\alpha a_2 a_5 f_l'' \\ & + Ec\alpha a_2 a_4 f_l''' + 2EcMa_4 f_l' + 4Eca_3 f_l''. \end{aligned} \tag{56}$$

where $q\epsilon[0,1]$ is the embedding parameter and $\bar{f}(\eta,q)$, $\bar{\theta}(\eta,q)$ are the unknown functions. The zeroth order deformation equation is given by:

$$(1-q)L_f[\bar{f}(\eta;q) - f_l(\xi)] = q\hbar_f N_f[\bar{f}(\xi;q),\bar{\theta}(\xi,q)] - H_1,$$

$$(1-q)L_\theta[\bar{\theta}(\eta;q) - \theta_l(\xi)] = q\hbar_\theta \bar{f}(\eta,q),\theta(\eta,q) - H_2.$$

Where $\hbar_f, \hbar_\theta$ are nonzero convergence controlling auxiliary parameter and $N_{\bar{f}}$ and N_θ are nonlinear operations given by:

$$N_f[\bar{f}(\eta,q),\bar{\theta}(\eta,q)] = \alpha f f'' - f'^2 + 2\alpha f' f''' + f f'' + 2\alpha f''^2, \tag{57}$$

$$\begin{aligned} N_\theta[\bar{f}(\eta,q),\bar{\theta}(\eta,q)] = {} & f'\theta' - f'\theta - d_y f'\theta + EcMf'^2 + 2Ecf''^2 \\ & - Ec\alpha f' f''^2 - 2Ec\alpha a_3 f' f'' - Ec\alpha a_4 f''^2 \\ & + Ec\alpha f f'' f''' + Ec\alpha a_5 f f'' + Ec\alpha a_4 f f''' \\ & + Ec\alpha a_2 f'' f''' \end{aligned} \tag{58}$$

Differentiating the above equation m times with respect to q and then set $q=0$ and finally dividing the resulting equations by $m!$ yields the mth order deformation equations:

$$L_f[f_m(\xi) - X_m f_{m-1}(\xi)] = \hbar_f R_m^f, \tag{59}$$

$$L_\theta[\theta_m(\xi) - X_m\theta_{m-1}(\xi)] = \hbar_\theta R_m^\theta. \tag{60}$$

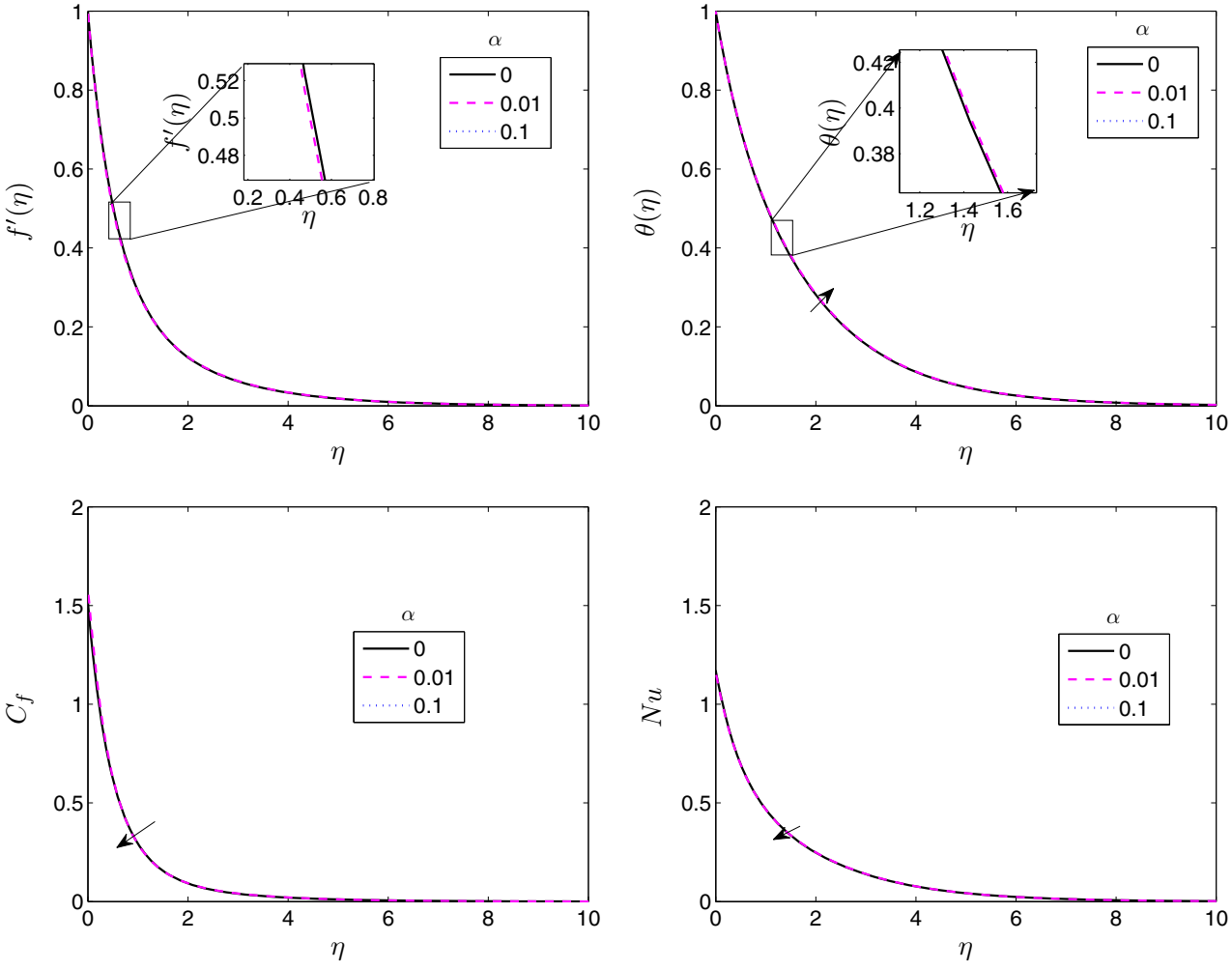

Figure 3 Influence of viscoelastic parameter α on velocity, temperature, skin friction coefficient and local Nusselt number profiles.

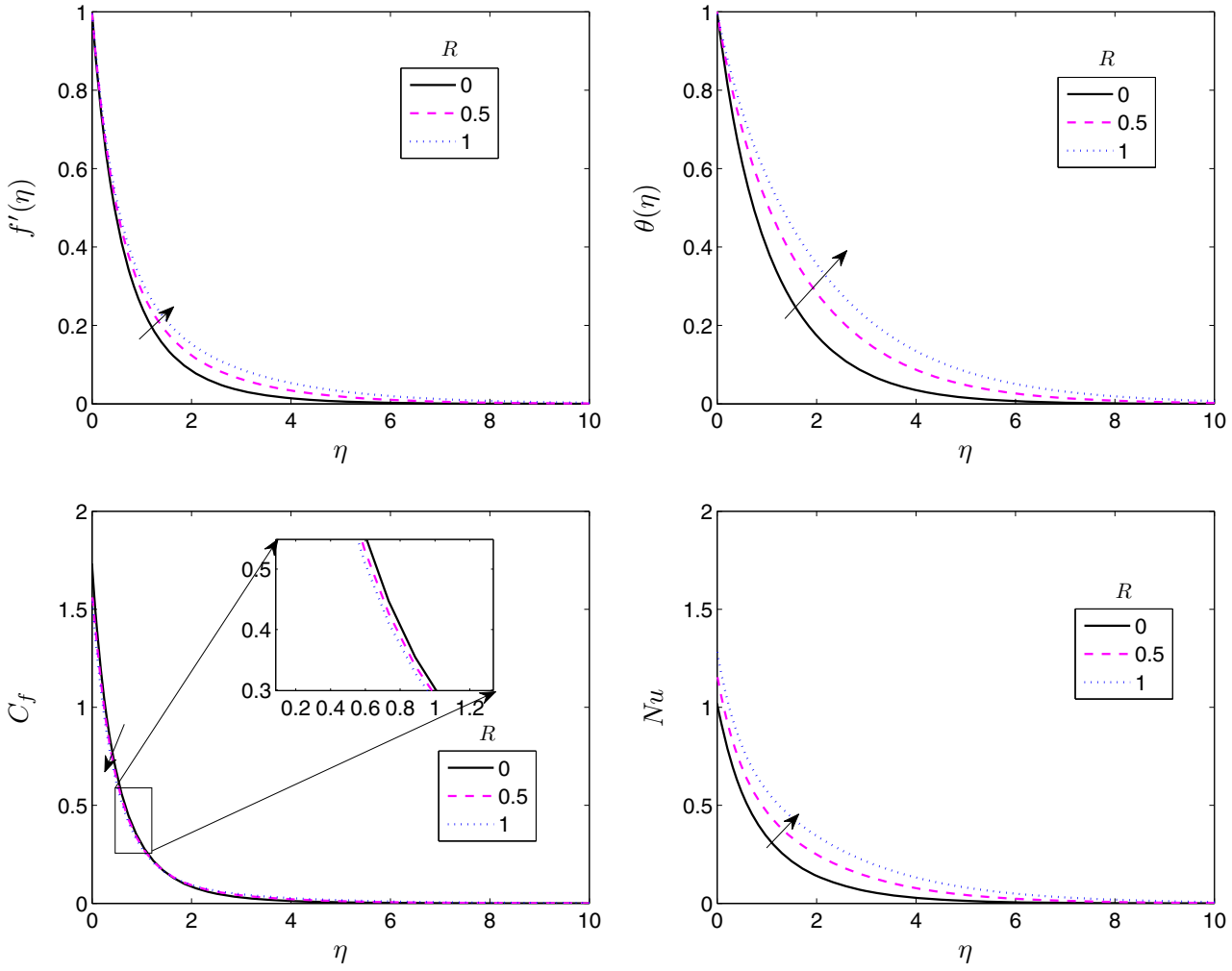

Figure 4 Influence of thermal radiation parameter R on velocity, temperature, skin friction coefficient and local Nusselt number profiles.

Subject to the boundary conditions:

$$f_m(-1) = f'_m(-1) = f'_m(1) = 0, \tag{61}$$

$$\theta_m(-1) = \theta_m(1) = 0. \tag{62}$$

where

$$\begin{aligned} R^f_m(\xi) = {} & f'''_{m-1} + \alpha a_1 f_{m-1} + \alpha a_2 f''''_{m-1} - 2a_4 f'_{m-1} - M f'_{m-1} + 2\alpha a_5 f'_{m-1} \\ & + 2\alpha a_4 f'''_{m-1} + Gr\theta_{m-1} + a_3 f_{m-1} + a_2 f''_{m-1} + 4\alpha a_3 f''_{m-1} \\ & + \sum_{n=0}^{m-1} \Big(\alpha f_n f''''_{m-1-n} + 2\alpha f'_n f'''_{m-1-n} + f_n f''_{m-1-n} - f'_n f'_{m-1-n} \\ & + 2\alpha f''_n f''_{m-1-n} \Big) - H_1(\eta)(1 - X_m), \end{aligned} \tag{63}$$

$$\begin{aligned} R^\theta_m(\xi) = {} & \frac{1}{Pr}(1+R)\theta''_{m-1} + b_1 f_{m-1} + b_2 \theta'_{m-1} - b_3 f'_{m-1} \\ & - b_4 \theta'_{m-1} - d_y b_3 f'_{m-1} - d_y b_4 \theta_{m-1} + A_{m-1} \\ & + \sum_{n=0}^{m-1} (f_n \theta'_{m-1-n} - f'_n \theta_{m-1-n} - d_y f'_n \theta_{m-1-n} + EcMf'_n f'_{m-1-n} \\ & + 2Ecf''_n f''_{m-1-n} - 2Ec\alpha a_3 f'_n f''_{m-1-n} - Ec\alpha a_4 f''_n f''_{m-1-n} + Ec\alpha a_5 f_n f'_{m-1-n} \\ & + Ec\alpha a_4 f_n f'''_{m-1-n} + Ec\alpha a_2 f''_n f''_{m-1-n}) \\ & + \sum_{i=0}^{n} \sum_{n=0}^{m-1} \left[Ec\alpha f_i f''_{n-i} f'''_{m-1-n} - Ec\alpha f'_i f''_{n-i} f''_{m-1-n} \right] - H_2(\eta)(1 - X_m). \end{aligned} \tag{64}$$

Applying the Chebyshev pseudo-spectral transformation on above gives;

$$Af_m = (X_m + \hbar) Af_{m-1} - \hbar(1 - X_m)G + \hbar Q_{m-1} \tag{65}$$

Subject to the boundary conditions:

$$f_m(\xi_N) = 0, \quad f_m(\xi_0) = 0, \tag{66}$$

$$\theta_m(\xi_N) = 0, \quad \theta_m(\xi_0) = 0. \tag{67}$$

where A and G are defined above, $F_m = [f_m(\xi_0), f_m(\xi_1), \ldots, f_m(\xi_N), \theta_m(\xi_0), \theta_m(\xi_1), \ldots, \theta_m(\xi_N)]^T$ and

$$\begin{aligned} Q_{1,m-1} = {} & \sum_{n=0}^{m-1} [\alpha f_n (D^4 f_{m-1-n}) + 2\alpha (Df_n)(D^3 f_{m-1-n}) + (f_n)(D^2 f_{m-1-n}) \\ & - (Df_n)(Df_{m-1-n}) + 2\alpha (D^2 f_n)(D^2 f_{m-1-n})] \end{aligned} \tag{68}$$

$$\begin{aligned} Q_{2,m-1} = {} & \sum_{n=0}^{m-1} ((f_n)(D\theta_{m-1-n}) - (Df_n)(\theta_{m-1-n}) - d_y (Df_n)(\theta_{m-1-n}) \\ & + EcM(Df_n)(Df_{m-1-n} + 2Ec(D^2 f_n)(D^2 f_{m-1-n}) \\ & - 2Ec\alpha a_3 (Df_n)(D^2 f_{m-1-n}) - Ec\alpha a_4 (D^2 f_n)(D^2 f_{m-1-n}) \\ & + Ec\alpha a_5 f_n (Df_{m-1-n}) + Ec\alpha a_4 f_n (D^3 f_{m-1-n}) \\ & + Ec\alpha a_2 (D^2 f''_n)(D^2 f_{m-1-n})) \\ & + \sum_{i=0}^{n} \sum_{n=0}^{m-1} [Ec\alpha f_i (D^2 f_{n-i})(D^3 f_{m-1-n}) - Ec\alpha (Df_i)(D^2 f_{n-i})(D^2 f_{m-1-n})]. \end{aligned} \tag{69}$$

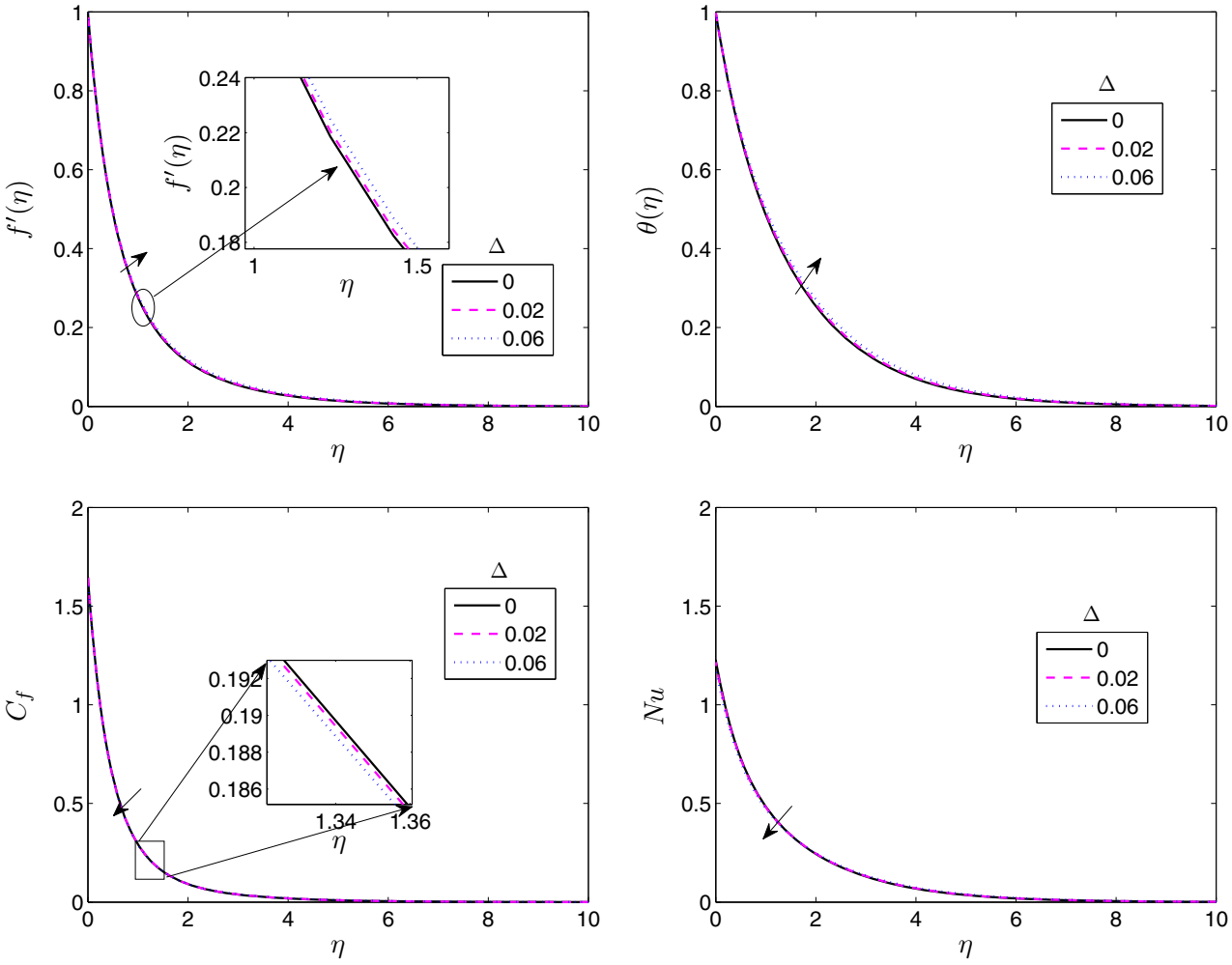

Figure 5 Effect of heat source or sink Δ on velocity, temperature, skin friction coefficient and local Nusselt number profiles.

The boundary conditions above are implemented on A on the left hand-side of rows 1, N, $(N+1)$ respectively as before with the initial solution above. The corresponding rows, all columns of A on the right hand-side G, $Q_{1,m-1}$, $Q_{2,m-1}$ are all set to zero. This results in the following recursive formular

$$F_m = (X_m + \hbar)A^{-1} \cdot \bar{A} f_{m-1} + \hbar A^{-1}[Q_{m-1} - (1 + X_m)G] \quad m \geqslant 1. \tag{70}$$

4. Results and discussion

The transformed ordinary differential Eqs. (28), (29), subject to the boundary conditions (30), (31), have been solved iteratively using a numerical version of the Homotopy Analysis Method (HAM), called Spectral Homotopy Analysis Method (SHAM) for some value of governing parameters i.e. the Grashof number Gr, the Hartmann number M, thermal radiation parameter R, suction/injection parameter β_0, heat absorption parameter and viscoelastic parameter α. SHAM is based on the blend of the Chebyshev pseudo-spectral method with the standard homotopy analysis method (HAM). For our computational analysis, we have set $Gr = 0.5$, $M = 0.5$, $Pr = 0.71$, $\alpha = 0.01$, $R = 0.5$, $d_y = 0.5$, $\Delta = 0.1$, $\beta_0 = -0.5$, $Ec = 0.01$ as standard values to compute table and plot graphs. All graphs therefore correspond to these values unless it is otherwise stated. In order to establish the accuracy of the present method of solution, we first deal with the special case of our problem and compare with literature results of Chamkha [10] and Acharya et al. [25] in Table 1. Table 1 illustrates the computational values of wall temperature gradient $-\theta'(0)$ for a special case of our model when pertinent parameters $\alpha = Gr = R = M = \Delta = 0$. The comparison shows that the present results by SHAM were in excellent agreement with the solution of Chamkha [10] and Acharya et al. [25]. Table 2 illustrates the effects of viscoelastic parameter α and Magnetic parameter M on both the skin friction coefficient C_f and local Nusselt number Nu of the flow respectively. It is observed that an increase in both Magnetic parameter M and viscoelastic parameter α of the Walter's B memory fluid causes a notable decrease in skin friction coefficient and local Nusselt number generation. Table 3 gives account on the effect of viscous dissipation term (i.e. Eckert number) and thermal Grashof number on the wall shear stress and local heat transfer rate when the flow is experienced possible heat generation and/or absorption. It is seen that with an increased thermal Grashof number and Eckert number on the flow, there is significant decrease and increase in skin friction coefficient and local Nusselt

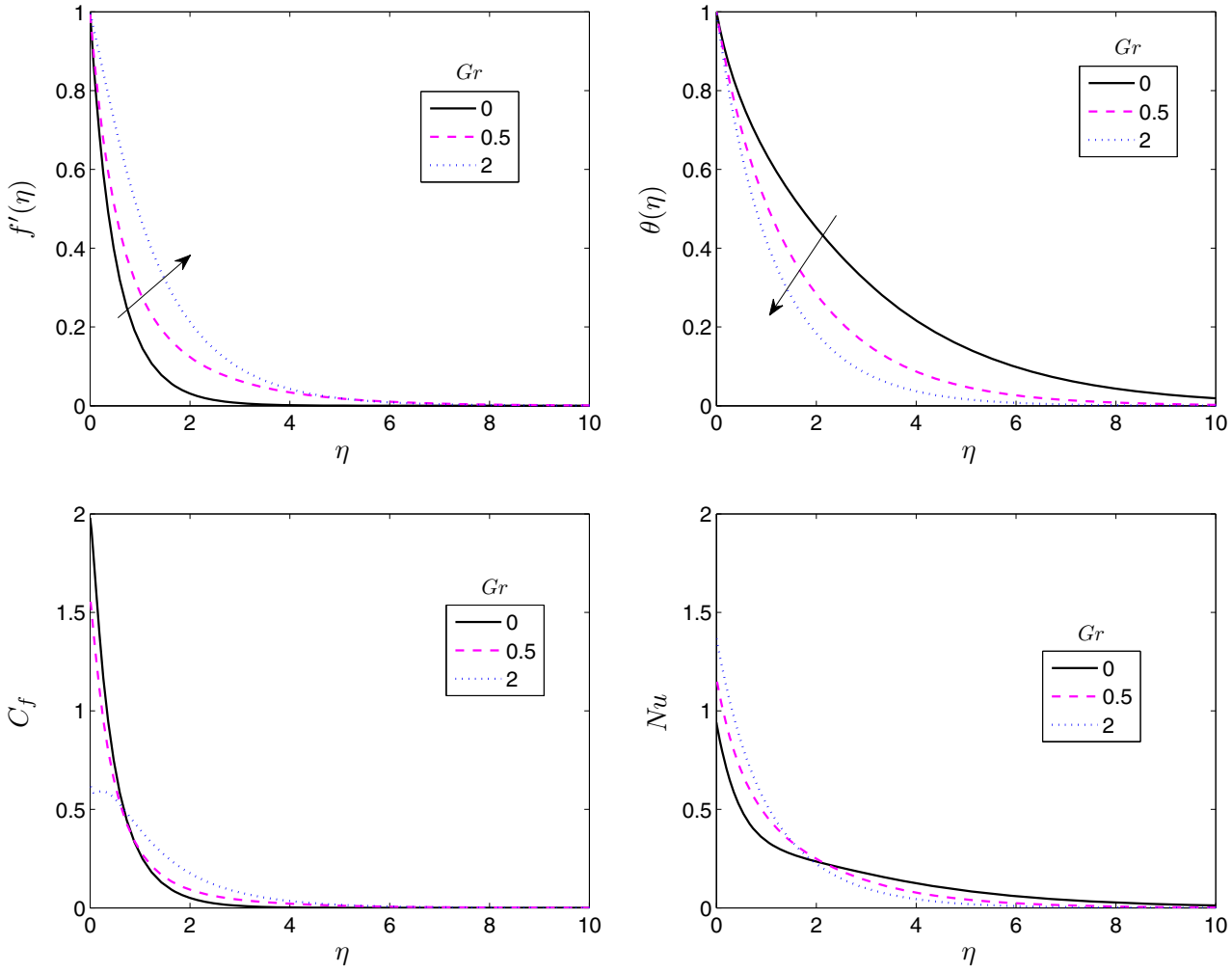

Figure 6 Effect of Grashof number Gr on velocity, temperature, skin friction coefficient and local Nusselt number profiles.

number respectively. To further illustrate the influence of the flow pertinent parameters on the fluid, we have shown graphically the effect of these parameters on the fluid velocity, temperature, skin friction coefficient and local Nusselt number profiles (see Figs. 2–8).

In Fig. 2, we present variation of Hartmann number M and its effects on the fluid velocity, temperature, skin friction and local heat transfer. We observe that an increase in the values of the Hartmann number as a result of the increasing effect of transverse magnetic field toward the electrically conducting fluid, leads to a remarkable reduction in the velocity and local heat transfer profile of the flow, whereas there is significant increase in both skin-friction coefficient and fluid temperature. Due to the damping effect of the magnetic field, increases in the values of M have a tendency to slow the motion of the fluid and make it warmer as it moves along the vertical plate causing the tangential velocity $f'(\eta)$ to decrease and the temperature $\theta(\eta)$ to increase. The transverse contraction on the velocity boundary layer of the flow is due to the applied magnetic field, which consequently invokes lorentz force producing noticeable opposition to the flow of the fluid and hence enhances the thermal condition (that is temperature profile). Therefore, magnetic parameter M influences the control of surface shear stress. Fig. 3 depicts the effect of viscoelastic parameter α (that is Weissenberg number) on the velocity, temperature, skin friction coefficient and local heat transfer profiles when other parameters are fixed. The viscoelastic parameter α represents the effect of normal stress coefficient on the flow. It is observed that at a given point on the flow domain, the flow velocity, skin friction coefficient and local heat transfer profiles decrease drastically with an increase in the viscoelastic parameter whereas an increase in viscoelastic parameter added value to the flow regime by significantly increasing the temperature distribution. This implies that an increase in viscoelastic parameter has tendency of decreasing the boundary layer thickness, while an increase in normal stress coefficient parameter has an opposing effect on the temperature profile of the flowing fluid. Fig. 4 gives account of variation of thermal radiation parameter (R) over the fluid velocity, temperature, skin friction and local heat transfer. The thermal radiation parameter R defines the relative contribution of conduction heat transfer to thermal radiation transfer. A noticeable increment in fluid velocity and temperature are observed as thermal radiation parameter increases whereas remarkable reduction and increment are noticed in skin friction and local heat transfer respectively. The results qualitatively agree with the report from the literature that one of the tangible effects of thermal radiation and surface temperature on flow is to enhance the rate of heat

Please cite this article in press as: Fagbade AI et al., MHD natural convection flow of viscoelastic fluid over an accelerating permeable surface with thermal radiation and heat source or sink: Spectral Homotopy Analysis Approach, Ain Shams Eng J (2016), http://dx.doi.org/10.1016/j.asej.2016.04.021

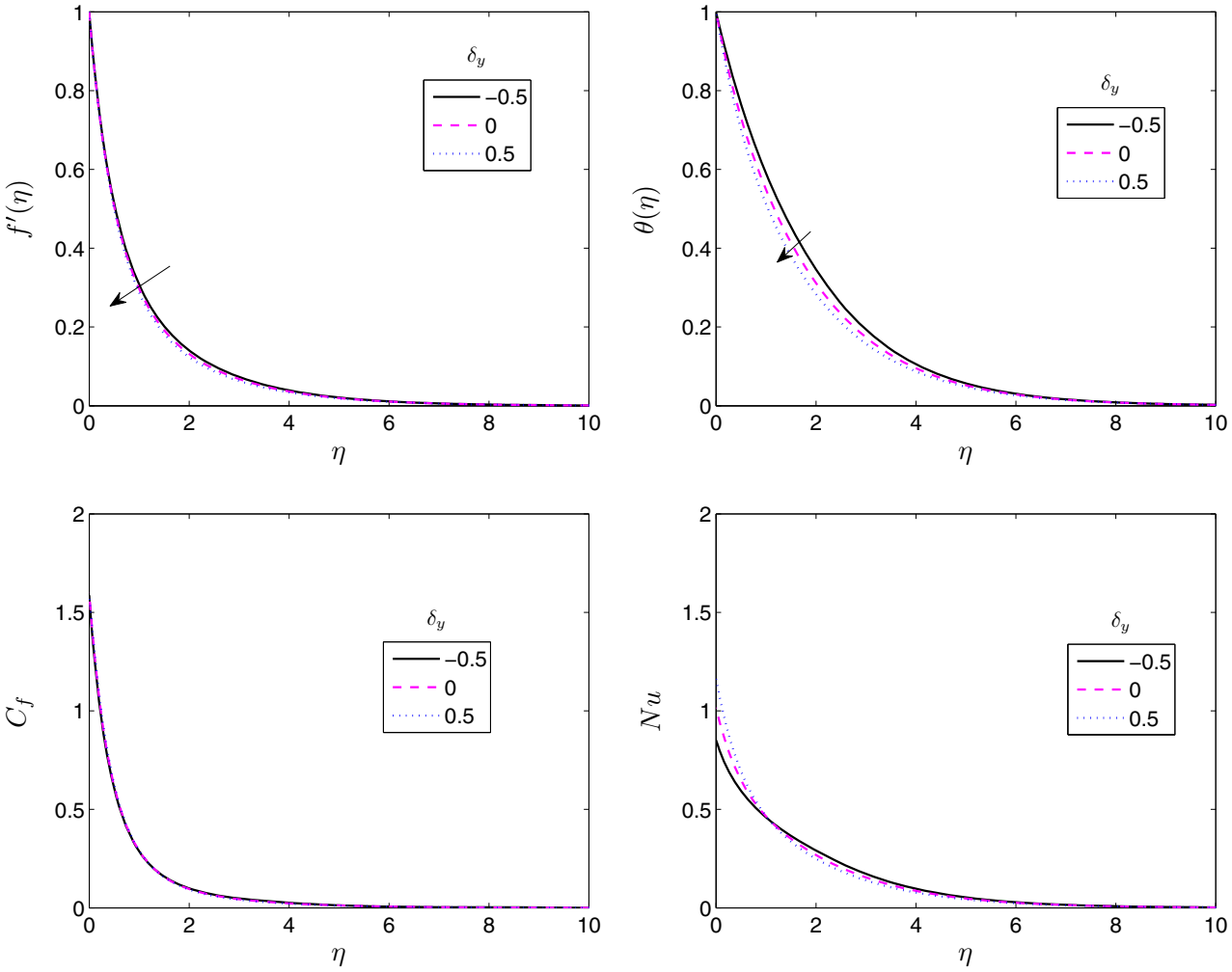

Figure 7 Effect of internal heat generation/absorption coefficient d_y on velocity, temperature, skin friction coefficient and local Nusselt number profiles.

energy transfer. Hence, one can easily control the rate of heat transfer characteristics using thermal radiation mechanism. Fig. 5 graphically illustrates the influence of heat source/sink (Δ) on the velocity, temperature, skin friction coefficient and local heat transfer profiles. The heat source adds more heat energy into the boundary layer flow. The generation of more heat energy significantly boosts the velocity and temperature profiles of the flow but reduces the amount of skin friction coefficient and local heat transfer within the boundary layer regime of the flow. The influence of thermal Grashof number on the flow profile is illustrated in Fig. 6. Thermal Grashof number Gr approximates the ratio of the buoyancy to viscous force acting on a fluid. When the thermal Grashof number is high the boundary layer is laminar and vice versa. It is observed that an increase in thermal Grashof number actually add more thermal energy into the fluid molecules, loosen up the intermolecular forces within the fluid particles and thereby increases the velocity profile and local heat transfer of the fluid. On the other hand the fluid particle gathered more momentum as a result of increase in thermal Grashof number, additional heat is lost to the surrounding and thereby reduces the skin friction coefficient generated and the temperature profile decreases.

Fig. 7 depicts the influence of the heat generation/absorption coefficient d_y on the behavior of the velocity, temperature, local heat transfer and skin friction coefficient profiles. It is clear from Fig. 7 that, an increase in d_y help boost the tangential velocity $f'(\eta)$ as well as in the temperature distributions $\theta(\eta)$ of the fluid. This is expected since heat generation ($d_y > 0$) causes the thermal boundary layer to become thicker and the fluid particles get warmer. This enhances the effect of thermal buoyancy of the driving body force due to mass density variations which are coupled to the temperature distribution and therefore, increases the fluid velocity distribution. Similarly, there is positive and significant influence of heat generation/absorption coefficient on the skin friction coefficient and local heat transfer as a result of an increase in heat generation/absorption. Fig. 8 displays the effect of mass transfer coefficient, that is suction/injection parameter β_0 on the velocity, temperature, skin friction coefficient and local heat transfer rate profiles of the flow. The velocity and temperature profiles increase as mass transfer coefficient parameter increases along the flow regime. The imposition of the wall fluid injection increases the hydrodynamic boundary layer with significant increment in the fluid velocity. Also,

Please cite this article in press as: Fagbade AI et al., MHD natural convection flow of viscoelastic fluid over an accelerating permeable surface with thermal radiation and heat source or sink: Spectral Homotopy Analysis Approach, Ain Shams Eng J (2016), http://dx.doi.org/10.1016/j.asej.2016.04.021

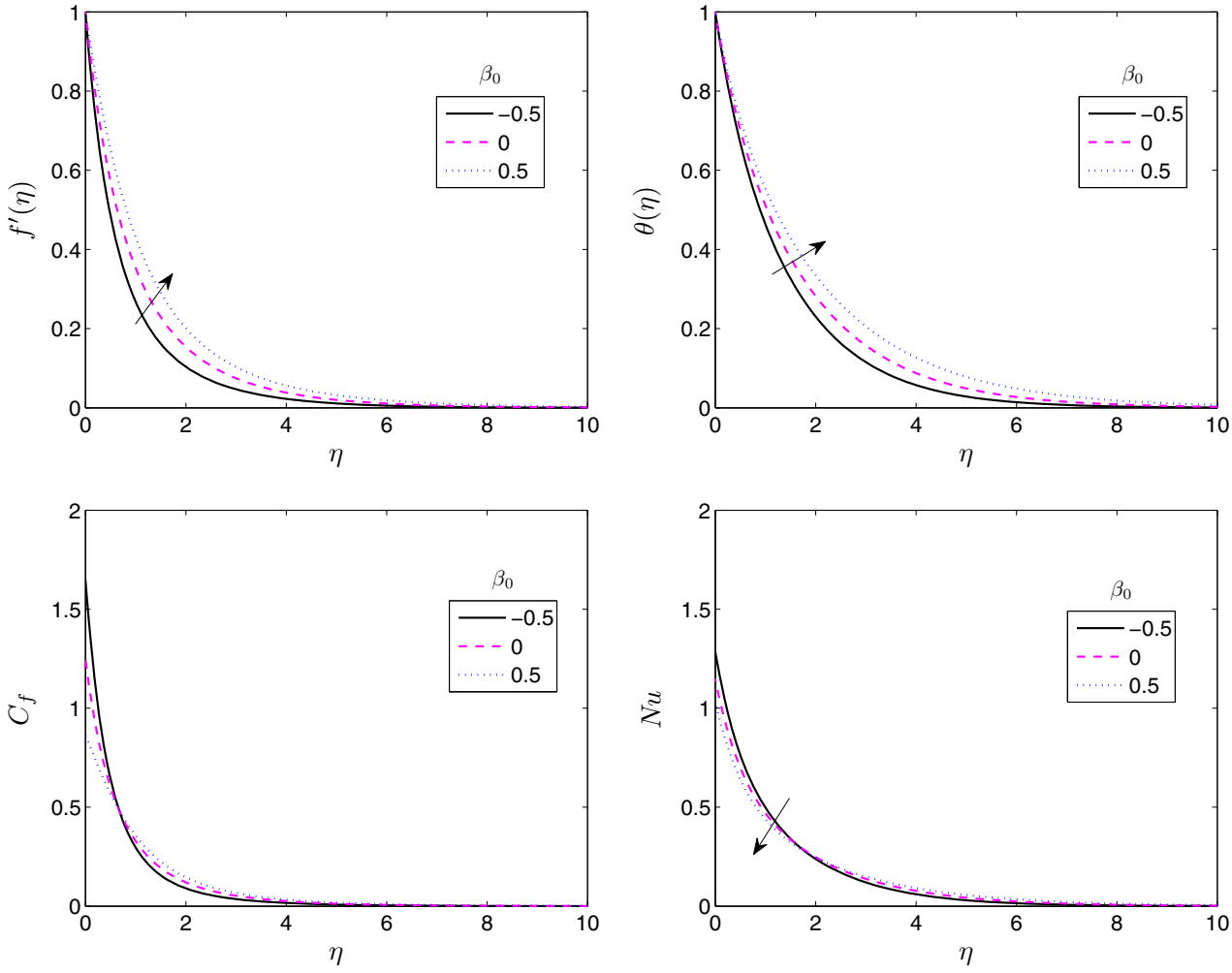

Figure 8 Influence of wall mass transfer coefficient β_0 at $\Delta = -0.1$ on velocity, temperature, skin friction coefficient and local Nusselt number profiles.

as the mass transfer coefficient parameter increases the temperature profile increases. On the other hand an increase in mass transfer coefficient reduces both the quantity of skin friction coefficient and local heat transfer rate within the boundary layer regime.

5. Conclusion

In this paper, we have used the Spectral Homotopy Analysis Method SHAM to solve a fourth-order nonlinear boundary value problem that governs the two-dimensional MHD natural convection flow of viscoelastic fluid over an accelerating permeable surface with thermal radiation and heat source or sink. Comparisons of the numerical results with previously published data for some special cases were made and found to be in excellent agreement. It is hoped that the present results be used for understanding more complex problems dealing with magnetohydrodynamic free convection flow of incompressible Walter's B memory fluid past a accelerating permeable surface plate. Our simulations show that the convergence of the SHAM solution series to the numerical solution up to five decimal place accuracy is achieved. The SHAM is apparently more efficient because it offers more flexibility in choosing linear operators compared to the standard HAM and other numerical methods reported in the reviewed literature. From our results we discovered that, when the Hartmann number M is increased the velocity profile decreases while temperature distribution increases. Also the velocity distribution decreases with an increase in the viscoelastic parameter. It was also found out that as the radiation parameter increases, the velocity as well as the temperature profile increases. Also, the heat source generates energy in the boundary layer while the heat sink absorbs energy and reduces the flow temperature.

References

[1] Chen CH. Heat and mass transfer in MHD flow by natural convection from a permeable, inclined surface with variable wall temperature and concentration. Acta Mech 2004;172:219–35.
[2] Ezzat M, El-Bary AA, Ezzat S. Combined heat and mass transfer for unsteady MHD flow of perfect conducting micropolar fluid with thermal relaxation. Energy Convers Manage 2011;52(2):934–45.
[3] Kalpadides VK, Balassas KG. Symmetry groups and similarity solutions for a free convective boundary-layer problem. Int J Non-linear Mech 2004;39:1659–70.

[4] Ibrahim FS, Mansour MA, Hamad MAA. Lie-group analysis of radiative and magnetic field effects on free convection and mass transfer flow past a semi-infinite vertical flat plate. Electron J Differ Eq 2005;39:1–17.
[5] Seigel R, Howell JR. Thermal radiation heat transfer. student ed.. Macgraw-Hill; 1971.
[6] Srihari K, Scrinivas Reddy G. Effects of radiation and soret in the presence of heat source/sink on unsteady MHD flow past a semi-infinite vertical plate. Brit J Math Comput Sci 2014(4):2536–56.
[7] Waqar AK, Zafar HK, Makinde OD. Non-aligned MHD stagnation point flow of variable viscosity nanofluids past a stretching sheet with radiative heat. Int J Heat Mass Transfer 2016;96:525–34.
[8] Makinde OD, Waqar AK, Richard CJ. MHD variable viscosity reacting flow over a convectively heated plate in a porous medium with thermophoresis and radiative heat transfer. Int J Heat Mass Transfer 2016;93:595–604.
[9] Magdy AE. Free convection effects on perfectly conducting fluid. Int J Eng Sci 2001;39(7):799–819.
[10] Chamkha AJ, Ahmed SE. Similarity solution for unsteady MHD flow near a stagnation point of a three dimensional porous body with heat and mass transfer, heat generation/ absorption and chemical reaction. J Appl Fluid Mech 2011;4(2):87–94.
[11] Seth GS, Ansari MdS, Nandkeolyar R. Effects of radiation and magnetic field on unsteady Couette flow in a porous channel. J Appl Fluid Mech 2011;4(2):95–103.
[12] Das SS, Biswal SR, Tripathy UK, Das P. Mass transfer effects on unsteady hydro magnetic convective flow past a vertical porous plate in a porous medium with heat source. J Appl Fluid Mech 2011;4(4):91–101.
[13] Raju MC, Varma SVK, Reddy NA. MHD thermal diffusion natural convection flow between heated inclined plates in porous medium. J Future Eng Technol 2011;6(2):45–8.
[14] Sharma PR, Singh G. Effects of variable thermal conductivity and heat source/sink on MHD flow near a stagnation point on a linearly stretching sheet. J Appl Fluid Mech 2009;2(1):13–21.
[15] Fagbade AJ, Falodun BO, U Boneze C. Influence of magnetic field, viscous dissipation and thermophoresis on Darcy–Forcheimer mixed convection flow in fluid saturated porous media. Am J Comput Math 2015(5):19–40.
[16] Waqar AK, Richard CJ, Makinde OD. Combined heat and mass transfer of third-grade nanofluids over a convectively-heated stretching permeable surface. Can J Chem Eng 2015;99 (10):1880–8.
[17] A Ezzat MA, Abd-Elaal MZ. State space approach to viscoelastic fluid flow of hydromagnetic fluctuating boundary-layer through a porous medium. ZAMM Zeitschrift fur Angewandte Mathematik und Mechanik 1997;77(3):197–207.
[18] Makanda G, Makinde OD, Sibanda P. Natural convection of viscoelastic fluid from a cone embedded in a porous medium with viscous dissipation. Math Prob Eng 2013;2013, 934712(11pages).
[19] Magdy AE, Abd-Elaal MZ. Free convection effects on a viscoelastic boundary layer flow with one relaxation time through a porous medium. J Franklin Inst 1997;334(4):685–706.
[20] Prasad KV, Pal D, Umesh V, Rao NSP. The effect of variable viscosity on MHD viscoelastic fluid flow and heat transfer over a stretching sheet. Commun Non-Linear Sci Numer Simul 2010;15:331–44.
[21] Mehmood A, Ali A, Shah T. Heat transfer analysis of unsteady boundary layer flow by homotopy analysis method. Commun Nonlinear Sci Numer Simul 2008;13(5):902–12.
[22] Walter K. Non-Newtonian effects in some elastico-viscous liquids whose behavior at some states of shear is characterized by general equation of state. Q J Mech Appl Math 1962;15:63–76.
[23] Chamkha AJ. Thermal radiation and buoyancy effects on hydromagnetic flow over an accelerating permeable surface with heat source or sink. Int J Eng Sci 2000(38):1699–712.
[24] Md Miraj A, Md Abdul A, Laek SA. Conjugate effects of radiation and joule heating on magnetohydrodynaics free convection flow along a sphere with heat generation. Am J Comput Math 2011;1:18–25.
[25] Acharya M, Singh LP, Dash GC. Heat and mass transfer over an accelerating surface with heat source in presence of suction and blowing. Int J Eng Sci 1999;37:189–211.

My name is **Fagbade Adeyemi Isaiah**. I am a self-motivated student with genuine interest in the Applied Mathematics. My research interest focuses on geophysical fluid dynamics, computational fluid dynamics with keen interest to learn more on modeling of fluid flow through a porous media and derivation of robust numerical methods and scientific computing for the applied problems that arise from interactions between flow and its environment as well as practical problems in engineering.
My research is a well-balanced combination of analytical investigations and numerical experiments using finite difference, spectral approach and other approximation methods. My current research entails the development of reliable numerical schemes for mathematical models arising in geothermal flow in porous media as well as other PDE problems.

Mr. Falodun B.O, is M.Tech scholar in Department of Mathematics, Federal University of Technology, Akure, Nigeria. His area of interest is boundary layer theory, computational fluid mechanics.

I am Dr. **Omowaye A.J**, a lecturer at the Federal University of Technology, Akure. I obtained Doctor of philosophy at Ladoke Akintola University of Technology, Ogbomoso, Nigeria. My area of interest is Boundary layer theory.

Please cite this article in press as: Fagbade AI et al., MHD natural convection flow of viscoelastic fluid over an accelerating permeable surface with thermal radiation and heat source or sink: Spectral Homotopy Analysis Approach, Ain Shams Eng J (2016), http://dx.doi.org/10.1016/j.asej.2016.04.021